JOURNAL OF SPACECRAFT AND ROCKETS
Vol. 41, No. 6, November–December 2004

Transpermanent Magnetic Actuation for Spacecraft Pointing, Shape Control, and Deployment

Larry Silverberg*
North Carolina State University, Raleigh, North Carolina 27695-7910
and
Dan Farmer†
Kenworth Truck Company, Kirkland, Washington 98033

Transpermanent magnetic actuators are systems consisting of one or more permanent magnets, some of whose magnetic strengths can be switched onboard by surrounding pulse-coils. Transpermanent magnetic actuators are shown to be particularly wellsuited for spacecraft pointing, shape control, and deployment applications. In many spacecraft pointing, shape control, and deployment applications, it is desirable to hold displacements or forces between two points to within specified requirements (the regulation problem) and periodically to change or remove these requirements (the tracking problem). Furthermore, the interest generally lies in satisfying the dynamic performance requirements while expending minimal power, while meeting tight tolerances (particularly in optical applications), and while experiencing little wear and fatigue. The transpermanent magnetic actuator is shown to expend no power during regulation, and the transpermanent magnetic actuator is shown to be able to change periodically or remove the strength of its own magnets, thereby enabling both fine-tune adjustments and large-scale adjustments during tracking. The fine-tune adjustments are necessary in thermally varying space environments, and the large-scale adjustments are necessary in deployment problems in which pivot points experience large-angle rotations. A transpermanent magnetic actuator concept is demonstrated.

Nomenclature

D	=	separation distance of the transpermanent magnetic (TPM) actuator in the constrained direction, m
d_r	=	separation distance for each magnet, r m
F_A	=	maximum actuator force, N
F_{ext}	=	total external force on actuator, N
F_s	=	force generated by scaling material, N
F_x	=	force generated by magnets in the direction of movement, N
k_A	=	equivalent stiffness of the actuator, N/m
k_e	=	pulse coil magnetic constant, N/m^2
k_p	=	permanent magnetic constant, N/m^2
k_{p_r}	=	permanent magnetic constant for each magnet, r, N/m^2
k_s	=	stiffness constant of the scaling material, N/m
L_{eq}	=	inductive properties for the pulse coil, (H)
x	=	separation distance of the TPM actuator in the direction of movement, m
x_t	=	transition point, m

I. Introduction

THE projected actuator requirements imposed on future spacecraft are more stringent than can be realized today.[1] One set of challenges arises as a result of the demand for larger, less massive optical surfaces, which pushes the limits of our pointing, shaping, and deployment capabilities. Larger spacecraft are more flexible, necessitating distributed regulation.[2] Systems employing distributed regulation can be inherently more reliable than today's systems because of the possibilities that arise associated with redundancy.[3] However, distributed regulation places a burden on spacecraft power systems and leads to the need for new deployment strategies that take advantage of distributed actuation. As spacecraft become larger and more flexible, optical requirements become particularly difficult to satisfy because new approaches to distributed sensing are also needed.

A comprehensive review of spacecraft actuators was performed elsewhere[4] and will not be attempted here. In past work by the authors, an approach to distributed actuation was employed that uses distributed electrostatic forces. The electrostatic forces naturally distribute themselves on surfaces, and the associated power requirements are low. The electrostatic forces can be attached to a rigid back surface,[5] or they can be attached directly to the flexible surface, thereby removing the need for a rigid back surface.[6] In independent works by several investigators, the electrostatic approach was demonstrated to be feasible, although the associated control authority can be low. Another approach to distributed actuation, which is a hybrid of permanent magnetic actuation and electromagnetic actuation, is called transpermanent magnetic (TPM) actuation. This paper discusses the merits of the TPM approach, and several designs are illustrated.

The central goal that motivates TPM actuation is to achieve the attractive characteristics exhibited by both permanent magnets and electromagnets simultaneously. Unpowered forces are created by permanent magnets during the hold state (regulation), and the changing state (tracking) is created by varying the magnetic strength of the permanent magnets by an onboard magnetization process.[7,8] This results in a set of attractive properties.

First is the property of soft locking: Hold-states are elastically maintained by forces between permanent magnets. When the forces exceed critical levels, the magnets separate rather than fail. Soft locking protects the actuators and the spacecraft from excessively large forces that could otherwise cause damage.

The second property is zero-power hold: In usual spacecraft applications, regulation is a continuous operation, and tracking is intermittent. The TPM consumes no power during regulation because the hold states are maintained by permanent magnets. This can reduce gross power requirements by several orders or magnitude or the need for latching type devices.[9]

Received 22 March 2003; revision received 24 July 2003; accepted for publication 13 August 2003.

*Professor, Mechanical and Aerospace Engineering; lmsilver@eos.ncsu.edu.
†Director, New Vehicle Programs, 10630 Northeast 38th Place; dan.farmer@paccar.com.

The third property is high-packaging density: The two largest components in a typical design of a TPM (as described later) consist of a pair of permanent magnets, one of which is surrounded by a pulsecoil. The pulse coil is used to change the state of the permanent magnet, which it surrounds. The state change is necessary when thermal loads vary or when functional requirements change (stationkeeping). The same pulse coil is used during deployment. During deployment, the pulse coil creates a short-duration electromagnetic force that can be an order magnitude greater than the permanent magnetic force. The electromagnetic force is used to initiate a large motion, launching the vehicle from a stowed configuration into a deployed configuration.

Fourth is the property of resolution: The resolution of the displacements and the range of motion are driven by a thin, thermally insensitive, elastic material, called the scaling material, that is placed between the two magnets. Depending on the elasticity of the scaling material, the TPM can be designed for such applications as a low-resolution solar shield or a high-resolution optical surface.

The fifth property is multiple equilibrium settings: In addition to possessing design flexibility in its resolution, the TPM can be designed to possess a set of equilibrium positions (settings) depending on the number of permanent magnets employed. The theoretical number of settings is shown to be 2^n, where n is the number of magnets.

The sixth property is the built-in sensor: Displacement and force measurements between the magnets can be determined from electrical impedance information associated with the circuit and the two magnets without the need for additional probes.

The last property is low wear and high reliability: Wear and fatigue of the actuator is inherently low in that the actuator, as much as 99% of the time, depending on the application, experiences no current flow. Part reduction as the result of the elimination of latching mechanisms reduces potential failure. Actuators can also be designed with no contact elements.

The next section of the paper describes the basic two-magnet concept of the TPM, followed by a generalization to the n-magnet TPM concept. The results provided in these and the following sections used a simplified representation of the magnetic force. The simplified representation of the magnetic force was compared to a precise representation of the magnetic force. Issues associated with resolution, stiffness settings, and deployment force and position feedback are discussed. A TPM concept is presented.

II. Two-Magnet TPM

As shown in Fig.1, a simple realization of a TPM consists of a fixed upper magnet surrounded by a pulse coil and a lower magnet that is free to move horizontally but constrained by an elastic scaling material. When a pulse from the electromagnet permanently changes the polarity of the upper magnet, the actuator will move to an equilibrium position that balances the magnetic force and the elastic force of the scaling material.

For the purposes of preliminary design, it is sufficient to represent the magnetic force by an inverse square law.[10] A comparison between the magnetic force obtained using the simplified inverse square law and the magnetic force obtained from a finite element

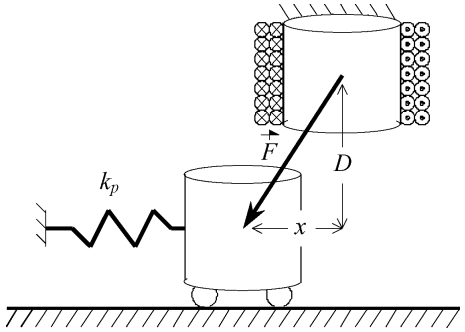

Fig. 1 Two-magnet TPM.

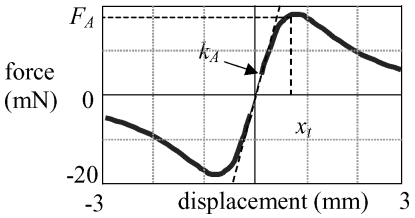

Fig. 2 Force vs displacement for two-magnet TPM, $k_p = 1$.

analysis is given in Sec. VII. The horizontal component of the magnetic force and the elastic force associated with the scaling material are

$$F_x = \left[k_p \Big/ \left(\sqrt{D^2 + x^2}\right)^2\right] \cdot \left(x \Big/ \sqrt{D^2 + x^2}\right) \tag{1a}$$

$$F_s = k_s x \tag{1b}$$

At equilibrium

$$k_s \cdot x \cdot (D^2 + x^2)^{\frac{3}{2}} + k_p \cdot x = 0 \tag{2}$$

Equation (2) admits four real and distinct equilibrium positions. There are two equilibrium positions at $x = 0$, which are stable when the magnets attract and metastable when the magnets repel. The two other equilibrium positions are equidistant from the origin. Thus,

$$x_1 = 0, \qquad x_{2,3} = \pm\sqrt{(k_p/k_s)^{\frac{2}{3}} - D^2} \tag{3}$$

As intuition would suggest, a larger separation distance D between the magnets decreases the actuator force and its movement, a larger magnetic stiffness k_p increases the movement, and a larger material stiffness constant k_s decreases the movement. The softness of the equilibrium position can be evaluated by replacing the spacing material with a varying external force, which yields

$$F_{\text{ext}} = -\left[k_p \Big/ (D^2 + x^2)\right] \cdot \left[x(D^2 + x^2)^{\frac{1}{2}}\right] \tag{4}$$

The softness is now apparent (Fig. 2).

For small displacements, the actuator behaves like a linear elastic spring. The slope k_A of the force/displacement curve at the equilibrium point represents the effective stiffness of the actuator. The transition point x_t represents the displacement, if exceeded, for which the actuator moves away to another equilibrium position. The corresponding force required to move the actuator to another equilibrium position is F_A. The external force of the actuator never exceeds F_A.

The force–displacement characteristics already described are well-suited for large space structures. During a space debris collision, for example, the softness of the actuator enables loads to be transferred throughout the system, thereby reducing peak stresses. After the collision, the system naturally returns to the original equilibrium position. In the event that an external force reaches the level of F_A, the actuator will move to another equilibrium position. The maximum external force that the spacecraft is subject to is bound above by F_A, not unlike, for example, an overcenter latch or a shear pin.

III. *N*-Magnet TPM

The two-magnet TPM has a single stable equilibrium position at a point where the magnets are aligned. Multiple equilibrium positions are achievable using more magnets. A simple realization of a multiposition actuator is shown in Fig. 3.

Extending the earlier formulation to n fixed magnets yields the equilibrium equation

$$0 = \sum_{r=0}^{n-1} \frac{k_{p_r} \cdot (d_r - x)}{\left[D^2 + (d_r - x)^2\right]^{\frac{3}{2}}} \tag{5}$$

When the magnets are uniform and have been magnetized to the same level, positive or negative, the constant k_p factors out of the

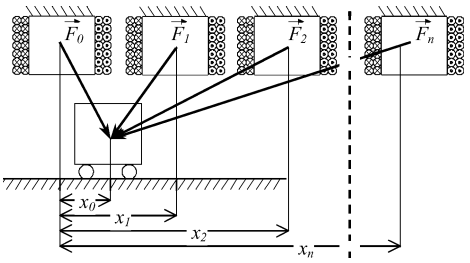

Fig. 3 Multiposition n-magnet TPM.

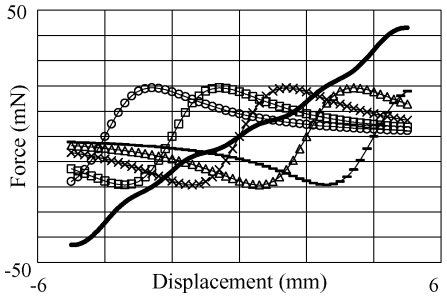

Fig. 4 Force vs displacement for five-magnet TPM, $k_1 = \cdots = k_5 = 1$: ○, magnet 1; □, magnet 2; ×, magnet 3; △, magnet 4; –, magnet 5; and ——, overall.

equation, leaving a positive or negative sign preceding each term depending on how the magnet is polarized. The number of combinations is 2^n, and so the n-magnet TPM has up to 2^n equilibrium positions. Like in the two-magnet TPM, some of the equilibrium positions can be repeated or physically unobtainable.

In Fig. 4, the polarities of all of the magnets are positive, causing the five-magnet TPM to behave like the two-magnet TPM with a higher maximum force, but with a lower effective stiffness and a wider operating range. Unlike the two-magnet TPM, the n-magnet TPM can exhibit a change in both stiffness and equilibrium characteristics. These characteristics can be exploited to create more complex force–displacement characteristics.

IV. Resolution and Stiffness Settings

Tuning Stiffness

The same TPM can be configured with different magnetic polarities producing a relatively hard holding force or a relatively soft holding force. The force–displacement curve of a five-magnet TPM is shown in Fig. 5, in which the stiffness k_A has been increased by reversing the polarity of the end magnets.

The same five-magnet TPM can produce four different levels of stiffness at the center by changing the off center magnets polarity in four symmetric combinations. Note also that the maximum force F_A in Fig. 5 is different from that in Fig. 4.

Tuning Equilibrium Positions

The equilibrium positions of the n-magnet TPM can be tuned by varying the relative strengths of the magnets. Figure 6 shows the force–displacement characteristics for a five-magnet TPM in which the polarization of one end magnet is reversed.

The five-magnet TPM can have up to 32 equilibrium positions. An actuator with five equal strength magnets has a maximum of 27 equilibrium positions because 5 are repeated at the center position.

Jumping

Actuator jumping is accomplished by changing the equilibrium positions of the permanent magnets. The jumping forces are produced by both the permanent magnets and the pulse coils so that they are inherently relatively large in magnitude. With a sufficiently small pulsing time constant, it is not difficult to create a force that is a magnitude larger than F_{ext} (Ref. 11), thereby initiating the jump. The pulse coil force can be treated like the permanent force in Eq. (4),

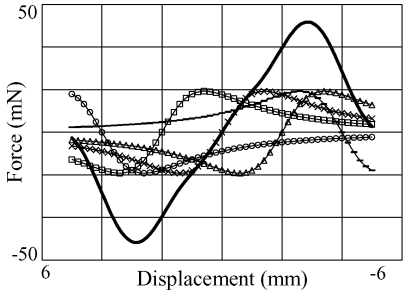

Fig. 5 Force vs displacement for five-magnet TPM with reversed polarization on the end magnets, $k_1 = k_3 = k_5 = -1$ and $k_2 = k_4 = 1$: ○, magnet 1; □, magnet 2; ×, magnet 3; △, magnet 4; –, magnet 5; and ——, overall.

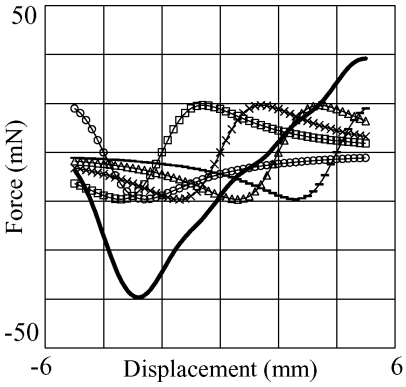

Fig. 6 Force vs displacement for five-magnet TPM with reversed polarization on one end magnet, $k_1 = -1$, and $k_2 = \cdots = k_5 = 1$: ○, magnet 1; □, magnet 2; ×, magnet 3; △, magnet 4; –, magnet 5; and ——, overall.

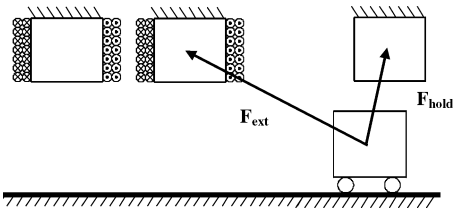

Fig. 7 Two-magnet TPM with third electromagnet for deployment.

in which case the total jumping force becomes

$$F_{\text{ext}} = -\left[k_p \big/ (D^2 + x^2)\right] \cdot \left[x \big/ (D^2 + x^2)^{\frac{1}{2}}\right] - \left[k_e \big/ (D^2 + x^2)\right] \cdot \left[x \big/ (D^2 + x^2)^{\frac{1}{2}}\right] \quad (6)$$

where k_e is the pulse coil force constant, which is typically larger than the permanent magnetic force constant k_p. During spacecraft deployment, the relatively large jumping force can be of particular value. A large repulsive jumping force can be utilized to initiate the deployment, sending the magnet into a large drifting state, after which a large attractive jumping force serves as a latching mechanism to terminate the deployment (Fig. 7). Notice that the deployment described scenario does not require additional hardware (latches and actuation) beyond that which is required for pointing and shape control.

V. Position Feedback

It is desirable to have a sensing capability of the force or the displacement between the magnets to be able to perform precision corrections. Toward this end, an inductive bridge circuit consisting of the TPM pulse coils can be used to measure the inductive impedance of the system[9] without the need for introducing additional transducers. For the four-magnet TPM shown in Fig. 3, a bridge circuit consisting of the pulse coils of the stationary TPMs was used to determine the position of the movable magnet. With use

of a typical bridge circuit equation,[10] the equivalent inductance of the pulse coils connected in series is

$$L_{eq} = [L_{1eq}/(L_{1eq} + L_{2eq})] - [L_{3eq}/(L_{3eq} + L_{4eq})] \qquad (7)$$

Unlike in magnetic suspension,[11] the magnets are motionless during the measurement in the TPM so that a small electric pulse must be applied to create an excitation source and the response measured. As the number of magnets increases, sensitivity can become a problem, in which case the magnet circuits could be grouped into multiple sets of no more than four magnets.[12]

VI. Illustrative Concepts

The following describes an illustrative concept in which a TPM actuator is designed for the Mars Exploration Surveyor Satellite's X-band, 8.4-GHz antenna dish. The dish is a 1.5-m (59-in.)-diam high-gain antenna that sits at the end of a 2.0-m (6.6-ft)-long boom (not the focusing length) attached to the propulsion module (Fig. 8). A gimbaled joint holds the antenna to the 0.714-m boom. The gimbaled joint actuator allows the antenna to automatically track and point at the Earth while science instruments observe Mars.

Working models of possible configurations for the TPM actuators needed for the earlier described models are shown in Fig. 9. Figure 9a shows the first working model that employs a minimal magnet design, and Fig. 9b shows the second higher resolution, working model with an increased number of magnets.

First Working Model

Setup

The TPM consists of eight magnets, nine switches, and one power source. In Fig. 9, 1 indicates the fixed base with four-magnet array, 2 the movable pendulum with four-magnet array, 3 the spherical joint, 4 and the magnetizer. The magnets were positioned in an orthogonal linear array, one four-magnet set on the base (equally spaced along the line in view) and a similar set on the end of a pendulum (not in view). In the configuration shown, there were 32 positions over a 22-deg range creating a 0.11 N · m (1.0 in. · lb) average rotational torque. The nonferrous actuator base was machined from polyvinyl chloride (PVC). The design goal of the shape of the base was to minimize magnet-to-magnet clearance and to maximize the holding force. The TPM permanent Alnico magnets were centered within pulse coils made from motor winding wires. A small amount of friction tape was wrapped around the magnet assembly to hold the magnets in place. The wires from the base of the unit were run through the back, into a bundle, and then attached to a terminal strip in the magnetizer. The wires from the movable magnet were fixed to the movable pendulum and the base. The wires were allowed to flex across the gimbaled joint.

Testing

A small laser pointer was attached to the pendulum. A paper was mounted to a surface above the actuator and was marked to indicate equilibrium positions. After determining the equilibrium positions, an unbalancing weight was placed on the pendulum to displace the actuator away from the equilibrium positions in a single direction. The measured displacements, unbalancing forces, and directions were used to determine actuator stiffness.

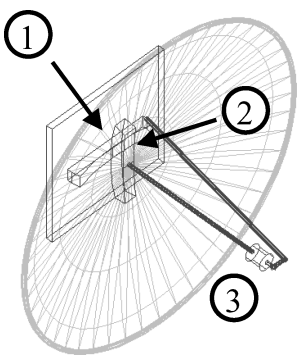

Fig. 8 Gimbaled joint TPM: 1) fixed base with magnet array, 2) movable pendulum with magnet array, and 3) joint.

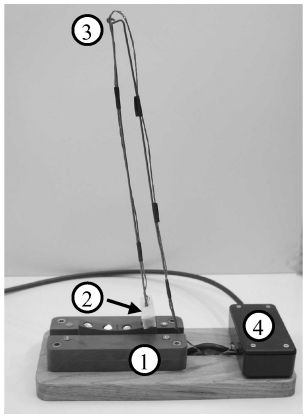

Fig. 9a First working model of revolute joint TPM: 1) fixed base with four-magnet array, 2) movable pendulum with four-magnet array, 3) spherical joint, and 4) magnetizer.

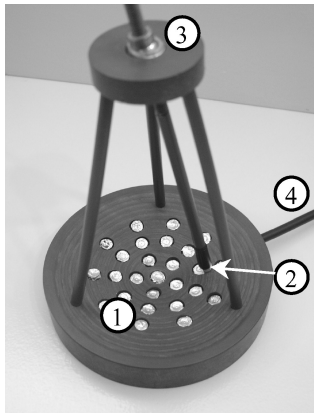

Fig. 9b Second working model of high-resolution revolute joint TPM: 1) 26-magnet array in base, 2) movable magnet at end of movable rod, 3) wires from magnetizer, and 4) spherical bearing.

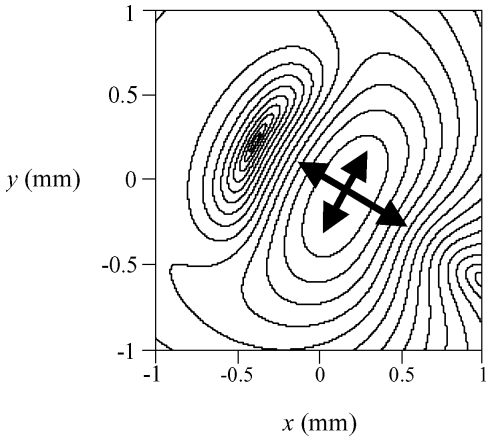

Fig. 10 Conformal map: 0.1 N · mm between contour lines, arrows in the direct of increasing force.

Analysis

The restoring force that is required to move the actuator to a given equilibrium position is represented using the contour map, shown in Fig. 10. The force sums to zero in all directions at the equilibrium position. The separation distance between contour lines indicates actuator stiffness.

Second Working Model

Setup

A second gimbaled-type actuator, shown in Fig. 9b, was constructed with the goal to achieve greater resolution and a larger number of equilibrium positions. In Fig. 9, 1 indicates the 26-magnet array in the base, 2 the movable magnet at end of movable rod, 3 the wires from magnetizer, and 4 the spherical bearing. This 26-magnet actuator can have 50,000 equilibrium positions. This design has a spherical ball joint that has a limited range of motion of 15 deg.

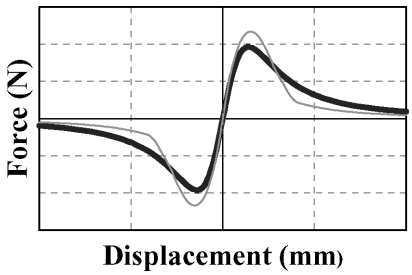

Fig. 11 Comparison of inverse square law with ANSYS model: ——, inverse square and ——, ANSYS model.

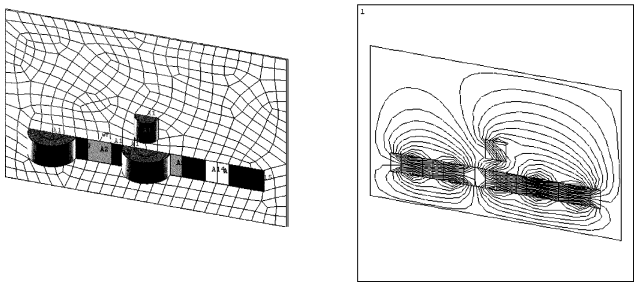

Fig. 12 Finite element analysis model showing flux lines defined on a plane through the axes of symmetry of a five-magnet actuator.

With closer magnet spacing, higher forces are generated with an average torque of 0.3 N · mm. The design of the cup shape of the base was determined from a rotated surface centered about the spherical joint. In this design, the gap between the movable and fixed magnets was quickly adjustable, allowing the adjustment of the equilibrium positions and force. All of the structure surrounding the TPM's and moving magnet were machined from PVC. In this design all electromagnets are in the base, and no wires run across the movable joint. In this 26-magnet design with one power source, 27 switches were needed.

Analysis

The same measurements were performed on the actuator to compare the actual stiffness and location of the equilibrium positions. Similar contour plots were generated for each location and gap between the movable and fixed magnets.

The power to change the state of either of the TPMs is a function of the actuator magnetic holding force. To change the state of the permanent magnet, the magnetic field of the pulse coil needs to be 3 or 4 times the PM field for a time sufficient to change the magnetic state of the PM. The actuator will have an efficiency advantage over an electromagnet actuator if the hold-state time well exceeds the state change of the PM.

Both actuators can be scaled. The actuator hold-state force scales with the volume of the permanent magnets. Smaller actuators are limited typically by current limitations of the pulse magnet and heat generation during state change. Because the repeatability of the actuator is a function of the frictional force in the flexible, sliding, or rotation joint, repeatability can decrease with scaling.

VII. Representation of Magnetic Forces

The analysis given in the paper represented the forces between permanent magnets by an inverse square law, when in fact magnetic forces are more complex than that; they are dependent on magnet geometry, nearby magnetic fields, and surrounding metals. Of course, the forces between permanent magnets can be more accurately modeled using available numerical analysis tools, ANSYS, for example. Figure 11 considers a two-magnet actuator. As shown, the level of accuracy that is achieved is sufficiently high for the purposes of a rudimentary analysis.

More complex models, such as the multiple-magnet actuators with close proximity of the magnets and complex pulsed magnetic fields, require numerical analysis. Figure 12 shows a five-magnet actuator magnetic flux path for one magnet configuration. Finite element programs such as ANSYS can be used to determine the actuator force in both the static hold state and the dynamically changing tracking state.

VIII. Summary

This paper showed that TPM actuation is a promising technology for pointing, shape control, and deployment in spacecraft applications. In addition to a general set of attractive properties listed, the paper also showed that TPM actuators possess multifunctional system-level properties that are attractive. The same TPM actuators that are used for pointing can be used for shape control and for deployment. No additional hardware is necessary for the sensing used in the feedback control. At the lower limit, scaling material can be used to prescribe the resolution of the pointing and shape control, whereas, at the upper the limit multiple TPM sets can be used to achieve a large range of motion. Furthermore, these system-level properties are scalable to large spacecraft. The resolution of the displacements is independent of the number and size of the spacecraft. The high packaging density should enable relatively large spacecraft to be deployed from relatively small, stowed configurations. A single power source supplies power to the TPMs, independent of their number. Although the development given in this paper of TPM technology for space applications has been verified experimentally, further work is needed to develop the actuator for a particular application, with all of its constraints, before the value of the approach can truly be confirmed.

References

[1]Horner, G., "NGST Actuator Concepts and Requirements," *Next Generation Space Telescope (NGST)*, NGST Cost and Process Integrated Product Team, NASA, Dec. 1998, p. 71.

[2]Silverberg, L., "Motion Control of Space Structures," *Journal of Aerospace Engineering*, Vol. 3, No. 4, 1990, pp. 223–234.

[3]Silverberg, L., "Uniform Damping Control of Spacecraft," *Journal of Guidance, Control, and Dynamics*, Vol. 9, No. 2, 1986, pp. 221–227.

[4]Fusaro, R. L., "Space Mechanism Needs for Future NASA Long Duration Space Missions," NASA TM-105204, 1991.

[5]Stanley, R., and Silverberg, L., "Paraboloidally Shaped Antenna Possessing Pointing and Beam-Width Control," *Journal of Spacecraft and Rockets*, Vol. 36, No. 5, 1999, pp. 736–744.

[6]Cromer, P., "Electrostatic Shaping of Structures Using Attached Control Surfaces," M.S. Thesis, Dept. of Mechanical and Aerospace Engineering, North Carolina State Univ., Raleigh, NC, 1995.

[7]Judy, J. W., Yang, H., Myung, N. V., Yang, C. K., Schwartz, M., and Nobe, K., "Integrated Ferromagnetic Micro-Sensors and Micro-Actuators," *Proceedings of the Fifth International Symposium on Magnetic Materials, Processes, and Devices*, Electrochemical Society, Pennington, NJ, 2000, pp. 456–468.

[8]Silverberg, L., and Duval, L., "Analysis of Trans-Permanent Magnetic Systems," *Journal of Dynamic Systems, Measurement and Control*, Vol. 125, No. 1, 2003, pp. 143–146.

[9]Ruan, M., Shen, J., and Wheeler, C., "Electronically Latching Micromagnetic Switches and Method of Operating Same," U.S. Patent 6,496,612, 17 Dec. 2002.

[10]Herceg, E. E., "Handbook of Measurement and Control: An Authoritative Treatise on the Theory and Application of LVDTs," Schaevitz Engineering, Rept. LCCC No. 76-24971, Pennsauken, NJ, May 1986.

[11]Skowronski, L., and Bisese, A., "Introduction to Magnetic Bearings," NASA, 1993.

[12]Frazier, R. H., Gilinson, P. J., Jr., and Oberbeck, P. J., *Magnetic and Electric Suspensions* MIT Press, Cambridge, MA, 1964.

D. Spencer
Associate Editor